Berry curvature and the anomalous Hall effect in Heusler compounds

Jürgen Kübler[1,*] and Claudia Felser[2]

[1]*Institut für Festkörperphysik, Technische Universität Darmstadt, D-64289 Darmstadt, Germany*

[2]*Institut für Anorganische Chemie und Analytische Chemie, Johannes Gutenberg–Universtität, D-55099 Mainz, Germany*

(Received 19 October 2011; revised manuscript received 12 December 2011; published 17 January 2012)

Berry curvatures are computed for a set of Heusler compounds using density functional calculations and the wave functions that they provide. The anomalous Hall conductivity is obtained from the Berry curvatures. It is compared with experimental values in the case of Co_2CrAl and Co_2MnAl. A notable trend cannot be seen but the range of values is quite enormous. The results for the anomalous Hall conductivities and their large variations as well as the degree of the spin polarization of the Hall current can be qualitatively understood by means of the band structure and the Fermi-surface topology.

DOI: 10.1103/PhysRevB.85.012405 PACS number(s): 75.10.Lp, 75.47.Np, 75.70.Tj

In connection with the emerging field of spintronics,[1] the anomalous Hall effect (AHE) is presently receiving new attention. The AHE in ferromagnets was explained long ago by Karplus and Luttinger,[2] who invoked spin-orbit coupling and perturbation by the applied electric field to expose an additional term to be added to the usual electron velocity. Rather recently,[3] this additional term was discovered to be related to the Berry curvature[4] in momentum space. It is an important correction to all transport properties[5] that rely on velocity. In particular, it describes the leading contribution to the AHE.[6]

Heusler compounds, especially those based on Co, with their regularities in many physical properties such as the Slater-Pauling behavior,[7,8] invite the question of whether such regularities are also present in the AHE. This is one of the questions we turn to here. Furthermore, a considerable number of Heusler compounds are half-metallic ferromagnets, i.e., they are gapped in one spin channel.[9] Therefore, in notable applications one tries to make use of spin currents, for which our calculations can serve as guidelines in estimates of the degree of spin polarization of the current.

The Berry curvature follows from the Berry vector,

$$\mathcal{A}(\mathbf{k}) = i \sum_n \langle u_{\mathbf{k},n} | \nabla_k | u_{\mathbf{k},n} \rangle, \tag{1}$$

where $u_{\mathbf{k},n}(\mathbf{r})$ is the crystal-periodic eigenfunction having wave vector $\mathbf{k}$ and band index n. The sum extends over the occupied states, which for metals vary with $\mathbf{k}$. The Berry curvature is written as

$$\Omega(\mathbf{k}) = \nabla_{\mathbf{k}} \times \mathcal{A}(\mathbf{k}). \tag{2}$$

It is obviously gauge-independent, in contrast to the Berry vector. The Berry curvature can be calculated in different ways. The common procedure is via a Kubo-like approach, where one calculates essentially a Green's function; see, e.g., Yao *et al.*[10] and more recently Lowitzer *et al.*[11] The other, less common, approach is via the wave functions directly, which, together with a fast band-structure method such as the linear muffin-tin orbital (LMTO) of Andersen,[12] is extremely efficient.

The numerical treatment used here to calculate Ω is basically a finite-difference approach. Some details may be summarized using Refs. 13–16 as follows. One begins by computing the so-called link-variable,[13]

$$U_{\mathbf{j}}(\mathbf{k}) = \det[\langle u_{n\mathbf{k}} | u_{m\mathbf{k}+\mathbf{j}} \rangle], \tag{3}$$

where the determinant is evaluated for the occupied states n and m. The component of $\mathcal{A}(\mathbf{k})$ along $\mathbf{j}$ is then

$$\mathcal{A}_{\mathbf{j}}(\mathbf{k}) = \mathrm{Im} \ln U_{\mathbf{j}}(\mathbf{k}), \tag{4}$$

which yields by finite differences for the z component of the Berry curvature (except for a scaling factor)

$$\Omega_z(\mathbf{k}) = \mathrm{Im} \ln \frac{U_y(\mathbf{k} + \hat{\mathbf{k}}_{\mathbf{x}}) U_x(\mathbf{k})}{U_y(\mathbf{k}) U_x(\mathbf{k} + \hat{\mathbf{k}}_{\mathbf{y}})}. \tag{5}$$

The logarithm implies that the results are mod 2π.

The Heusler compounds of interest here are face-centered-cubic possessing L_{21} symmetry, except for Mn_2PtSn, which is tetragonal with space-group no. 119. They are ferromagnetic; time-reversal symmetry is therefore broken, which leads to a nonzero Berry curvature.[5,6]

The wave functions are calculated in the local density-functional approximation (LDA)[17] using the augmented spherical wave (ASW)[18] method, which, just like Andersen's LMTO,[12] is extremely fast and efficient. The bispinor functions are expanded inside the atomic spheres using a minimal basis composed of numerical solutions of the Schrödinger equation and spherical harmonics.[12,18] Spin-orbit coupling (SOC), which is essential for this theory, is included in a second variation.[19]

The anomalous Hall conductivity, σ_{xy}, is given by the Berry curvature as

$$\sigma_{xy} = -\frac{e^2}{\hbar} \frac{1}{N} \sum_{\mathbf{k} \in (\mathrm{BZ})} \Omega_z(\mathbf{k}) f(\mathbf{k}), \tag{6}$$

where $f(\mathbf{k})$ is the Fermi distribution function, $\Omega_z(\mathbf{k})$ is the z component of the Berry curvature for the wave vector $\mathbf{k}$, N is the number of electrons in the crystal, and the sum extends over the Brillouin zone (BZ).

In the figures to be presented, the z component of the Berry curvature is shown in a cut through the fcc BZ; this was chosen to be the $k_z = 0$ plane. While the number of k points (441) to obtain these figures could be chosen sufficiently large for the plots to show significant details, yet being small enough to use

TABLE I. Collection of experimental and calculated data relevant for the Hall conductivity. N_V is the number of valence electrons, a is the lattice constant, M^{exp} is the experimental and M^{calc} the calculated magnetic moment in μ_B, σ_{xy} is the Hall conductivity in $(\Omega\,\text{cm})^{-1}$, calculated by means of Eq. (6), and P is an estimate of the spin polarization of the Hall current.

Compound[a]	N_V	a (nm)	M^{exp}	M^{calc}	σ_{xy}	P (%)
Co_2VGa	26	0.5779	1.92	1.953	66	65
Co_2CrAl	27	0.5727	1.7	2.998	438	100
Co_2VSn	27	0.5960	1.21	1.778	−1489	35
Co_2MnAl	28	0.5749	4.04	4.045	1800	75
Rh_2MnAl	28	0.6022		4.066	1500	94
Mn_2PtSn[b]	28	0.4509 (1.3477)		6.66	1108	91
Co_2MnSn	29	0.5984	5.08	5.00	118	82
Co_2MnSi	29	0.5645	4.90	4.98	228	100

[a]Experimental data from J. Winterlik (private communication) and compilations in Ref. 8.

[b]Tetragonal, space-group no. 119, c/a ratio in parentheses.

a notebook for the calculations, the Hall conductivity σ_{xy} at $T = 0$ K, which was calculated by means of Eq. (6), needed very large numbers of k points for convergence. Our results are converged to within about 20%, with approximately 2000 points in the irreducible wedge of the BZ.

Haldane[20] showed that Fermi-liquid theory is still valid even though it appears that the Hall conductivity, Eq. (6), depends on all states below the Fermi energy. He showed that the Berry curvature can be transformed to the Berry phase on the Fermi surface only. Thus an alternative to our calculations exists.[6,21] This is a transformation to Berry phases on the Fermi surface, but it requires special techniques to handle the three-dimensional surfaces. Our calculations, in contrast, are indeed quite straightforward. The results of our calculations are collected in Table I, where an estimate, P, of the degree of spin polarization of the Hall current is also given. This is obtained by counting the number of majority-spin electron states within 40 meV (arbitrarily chosen) below the Fermi energy, N^+, in the irreducible wedge of the BZ, and similarly the number of minority-spin states, N^-, then $P = N^+/(N^+ + N^-)$. These numbers are given by $N^\pm = \sum_{\mathbf{k}} n^\pm(\mathbf{k})$, where the spin-resolved norms, $n^\pm(\mathbf{k})$, are either 0 or 1 if SOC is ignored, but SOC mixes into a given spin state contribution of the opposite spin, thus a "spin filter" finds the $n^\pm(\mathbf{k})$ larger than 0 or smaller than 1. No broadening was used for the determination of $n^\pm(\mathbf{k})$.

Starting with the valence electron number $N_V = 26$, the Hall conductivity is calculated for Co_2VGa and is given in Table I. The Berry curvature for Co_2CrAl with $N_V = 27$ valence electrons is shown in Fig. 1 and the integrated value is given in Table I. All states within 40 meV below the Fermi energy are majority-spin states. This agrees with the value of P given in the table. The density of states of Co_2CrAl shown in Fig. 2 also agrees with $P = 100\%$. The features to be noticed in Fig. 1 are the large positive and negative peaks near the X and W points, respectively. They are caused by Fermi-surface sections. It is seen that the positive values dominate, which is in line with the integrated value of $\sigma_{xy} = 438$ $(\Omega\,\text{cm})^{-1}$ give in the table. There is an experimental

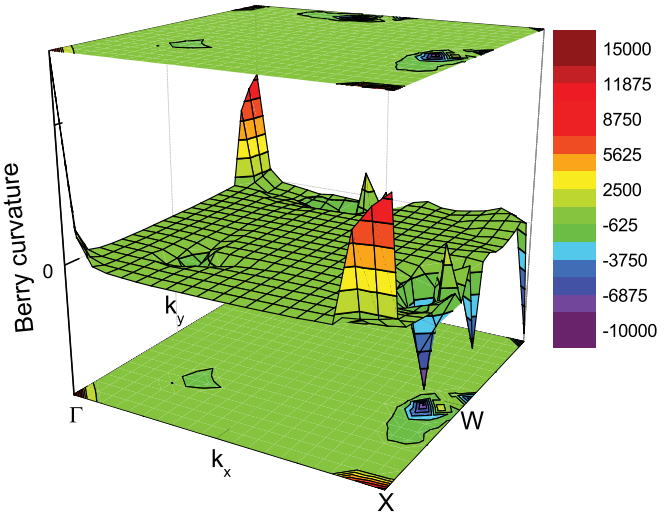

FIG. 1. (Color online) The Berry curvature in the $k_z = 0$ plane for Co_2CrAl. The color codes are in units of $(\Omega\,\text{cm})^{-1}$. The labels follow the standard notation for the face-centered-cubic crystal. The Berry curvature is entirely due to majority-spin electrons. Top and bottom show projections.

value[22] of $\sigma_{xy} = 125$ $(\Omega\,\text{cm})^{-1}$ to be compared with our value. The difference is significant, but the rather low value measured for the magnetic moment of $1.7\mu_B$ cannot be explained by our density of states shown in Fig. 2, which results in a magnetic moment of $3\mu_B$. The reason is most likely that the sample is disordered and does not have the ideal Heusler L_{21} crystal structure. Furthermore, it is possible but less likely that the other contributions to the Hall effect, i.e., side jump-and-skew scattering mechanisms, contribute considerably here.[6]

The Heusler compound Co_2VSn also with $N_V = 27$ valence electrons is not a half-metallic ferromagnet[8] having a measured moment of $1.21\mu_B$ and a calculated one of $1.78\mu_B$. In Fig. 3, we show the Berry curvature in the $k_z = 0$ plane as a projection only. The band structure reveals in Fig. 4 a Dirac cone below the Fermi energy describing minority-spin electrons. This cone disappears when SOC is neglected. These states show up in the Berry curvature as the semicircle and the white dots around

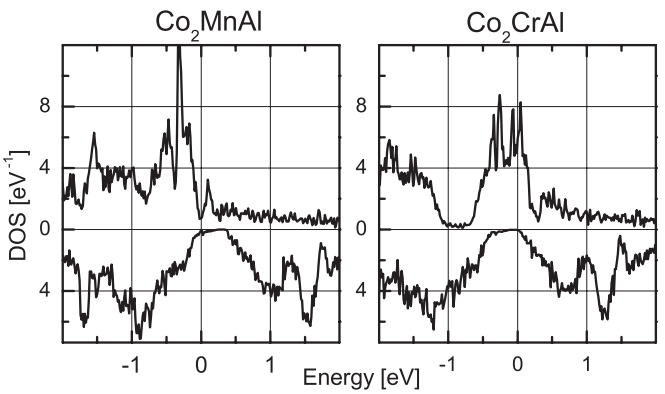

FIG. 2. Density of states of Co_2MnAl and Co_2CrAl. The upper parts of the figure describe majority-spin electrons and the lower parts describe minority-spin electrons. In contrast to spin up and down, these terms are well defined even in the spin-orbit coupled systems.

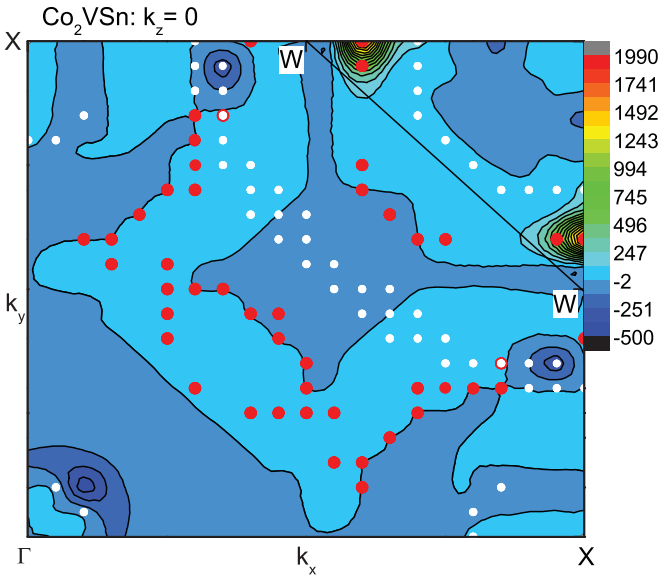

FIG. 3. (Color online) The Berry curvature in the $k_z = 0$ plane for Co_2VSn. Color code and labels as in Fig. 1. The red and white dots mark band energies of majority-spin and minority-spin electrons, respectively, within 40 meV below the Fermi energy.

the Γ point. The states seen near the W points are due to majority-spin electrons (red dots). The Dirac cone results in negative contributions to the Hall conductivity, while the other states give positive contributions resulting in a calculated Hall conductivity of $\sigma_{xy} = -1489\ (\Omega\,\mathrm{cm})^{-1}$ and a polarization of only 35%.

Next is Fig. 5 for Co_2MnAl with 28 valence electrons. The magnetic moment is measured and calculated to be $4.04\mu_B$. Here we obtain the high value of $\sigma_{xy} = 1800\ (\Omega\,\mathrm{cm})^{-1}$. In the density of states, Fig. 2, the Fermi energy sits in tails of states at the low-energy side of the gap, therefore we see minority-spin electrons in the Fermi surface near Γ and majority-spin electrons near X and W. The latter contribute positively to σ_{xy},

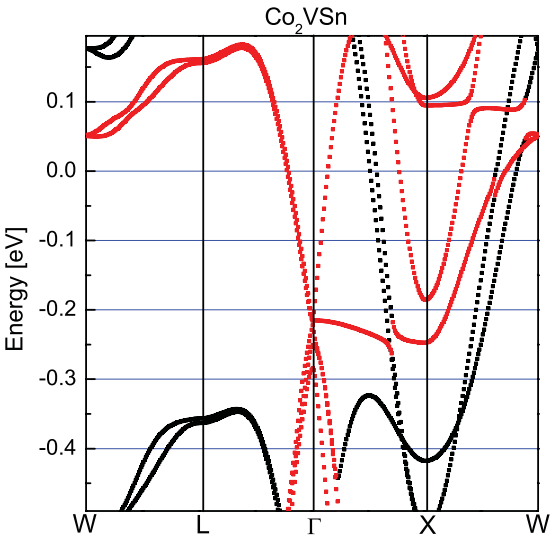

FIG. 4. (Color online) Band structure near the Fermi edge of Co_2VSn. Majority-spin electron states appear in red, minority-spin states in black. Note the Dirac cone at the Γ point at about −0.22 eV.

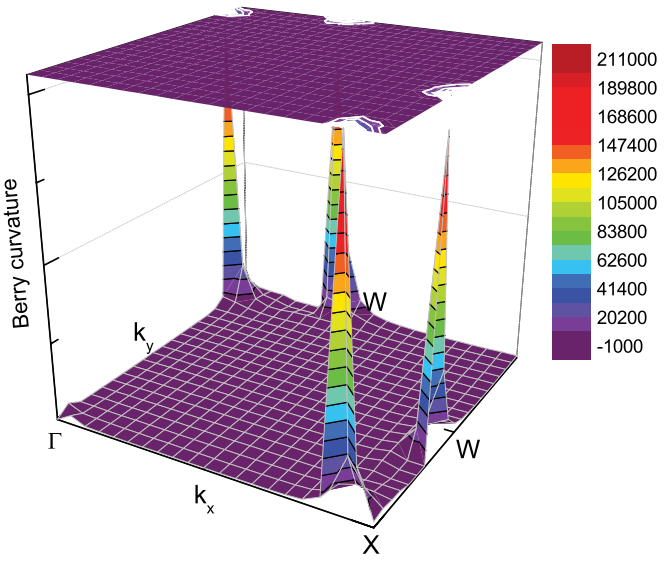

FIG. 5. (Color online) The Berry curvature in the $k_z = 0$ plane for Co_2MnAl. The small values near the Γ point originate from minority-spin electrons, the large peaks from majority-spin electrons.

while negative contributions originate from the former. The Fermi surface near Γ shows up in Fig. 5 as the small elevation near the origin. The large peaks indicate a large integrated value for σ_{xy}, but negative contributions in other parts of the BZ reduce the value considerably.

There is a recent study of the AHE for Co_2MnAl by Vidal *et al.*[23] that allows for an estimate of the Hall conductivity. If one takes their measured saturation value of the Hall resistivity of $\rho_{xy} \cong 20\ \mu\Omega\,\mathrm{cm}$ and their estimated specific resistivity of order of $100\ \mu\Omega\,\mathrm{cm}$, then the Hall conductivity is obtained to be approximately $2000\ (\Omega\,\mathrm{cm})^{-1}$. This could be considered to be in good agreement with the theory were it not for

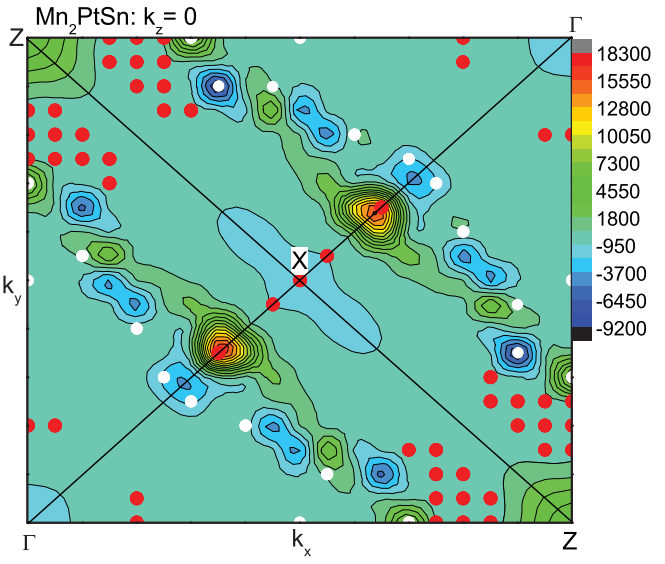

FIG. 6. (Color online) The Berry curvature in the $k_z = 0$ plane for tetragonal Mn_2PtSn. Color code and dots as in Fig. 3. The symmetry labels are the standard ones for the bct lattice.

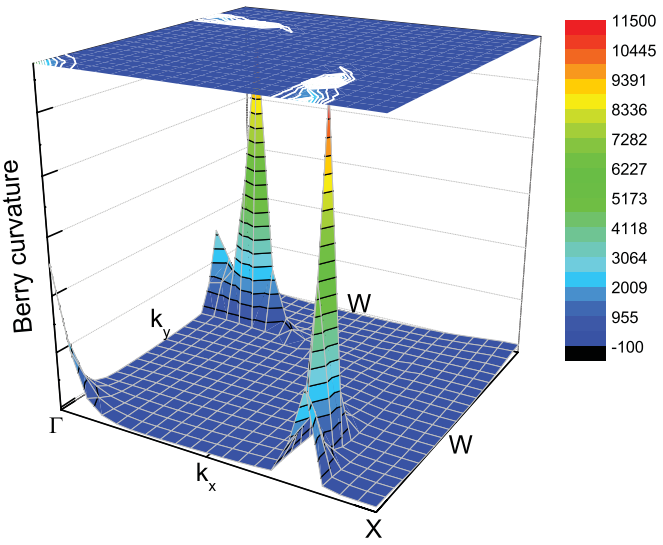

FIG. 7. (Color online) The Berry curvature in the $k_z = 0$ plane for Co_2MnSi. The entire structure is due to majority-spin electrons.

experimentally disordered Mn and Al sites in the samples, a fact that is stressed by Vidal *et al.*[23]

To guide the search for other ferromagnetic compounds with a large Hall conductivity, we enquired into the role of the strength of SOC. For this reason, we increased the SOC strength by 40% and found for Co_2MnAl a conductivity of $\sigma_{xy} = 2150\ (\Omega\,\mathrm{cm})^{-1}$. This increase originates from the states near X in Fig. 5. The increased role of SOC is realized in Rh_2MnAl through the heavier element Rh, for which, therefore, the Hall conductivity was calculated and found to be $1500\ (\Omega\,\mathrm{cm})^{-1}$. This is within the value obtained for Co_2MnAl but does not show the expected increase.

Since it is the valence electron number of $N_V = 28$ where the conductivity is especially large, we calculated the electronic structure of the tetragonal Heusler compound Mn_2PtSn, which also has 28 valence electrons. The Berry curvature is shown in Fig. 6 in a projection that allows for an easy comparison with Fermi-surface data. It is seen that the minority-spin states result in negative contributions to the Hall conductivity, the total (Table I) $\sigma_{xy} = 1108\ (\Omega\,\mathrm{cm})^{-1}$ being only reasonably large.

For Co_2MnSi, finally, the Berry curvature is shown Fig. 7. This compound has 29 valence electrons. It is a half-metallic ferromagnet having a measured magnetic moment of $4.90\mu_B$ that is calculated to be $4.98\mu_B$. The spin polarization of the Hall current is 100%; still, the Hall conductivity is only $\sigma_{xy} = 228\ (\Omega\,\mathrm{cm})^{-1}$. A comparison of Fig. 7 with Fig. 5 may be helpful to appreciate the difference between Co_2MnSi and Co_2MnAl, but the relatively low value of σ_{xy} is not obvious.

Summarizing, we state that strong trends such as the Slater-Pauling behavior are not seen in the Hall conductivity. However, large values of the Hall conductivity can be found in special cases such as Co_2MnAl and other systems having 28 valence electrons. The strength of SOC is shown to be but one ingredient to ensure large values of σ_{xy}, however a general rule still has to be found.

The generous supply of computer time by U. Nowak (Universität Konstanz) and the financial support by the DFG/ASPIMATT project (unit 1.2-A) are gratefully acknowledged.

*jkubler@fkp.tu-darmstadt.de

[1] S. A. Wolf, D. D. Awschalom, R. A. Buhrman, J. M. Daughton, S. von Molnár, M. L. Roukes, A. Y. Chtchelkanova, and D. M. Treges, Science **294**, 1488 (2001).
[2] R. Karplus and J. M. Luttinger, Phys. Rev. **95**, 1154 (1954).
[3] Z. Fang, N. Nagaosa, K. S. Takahashi, A. Asamitsu, R. Mathieu, T. Ogasawara, H. Yamada, M. Kawasaki, Y. Tokura, and K. Terakura, Science **302**, 92 (2003).
[4] M. V. Berry, Proc. R. Soc. London **392**, 45 (1984).
[5] D. Xiao, C. Chang, and Q. Niu, Rev. Mod. Phys. **82**, 1959 (2010).
[6] N. Nagaosa, J. Sinova, S. Onoda, A. H. MacDonald, and N. P. Ong, Rev. Mod. Phys. **82**, 1539 (2010).
[7] C. Felser, G. H. Fecher, and B. Balke, Angew. Chem. Int. Ed. **46**, 668 (2007).
[8] J. Kübler, G. H. Fecher, and C. Felser, Phys. Rev. B **76**, 024414 (2007).
[9] M. I. Katsnelson, V. Y. Irkhin, L. Chionel, and R. A. de Groot, Rev. Mod. Phys. **80**, 315 (2008).
[10] Y. Yao, L. Kleinman, A. H. MacDonald, J. Sinova, T. Jungwirth, D. S. Wang, E. Wang, and Q. Niu, Phys. Rev. Lett. **92**, 037204 (2004).
[11] S. Lowitzer, D. Ködderitzsch, and H. Ebert, Phys. Rev. Lett. **105**, 266604 (2010).
[12] O. K. Andersen, Phys. Rev. B **12**, 3060 (1975).
[13] T. Fukui and Y. Hatsugai, J. Phys. Soc. Jpn. **76**, 053702 (2007).
[14] R. D. King-Smith and D. Vanderbilt, Phys. Rev. B **47**, 1651 (1993).
[15] R. Resta, Rev. Mod. Phys. **66**, 899 (1994).
[16] D. Xiao, Y. Yao, W. Feng, J. Wen, W. Zhu, X.-Q. Chen, G. M. Stocks, and Z. Zhang, Phys. Rev. Lett. **105**, 096404 (2010).
[17] W. Kohn and L. J. Sham, Phys. Rev. **140**, A1133 (1965).
[18] A. R. Williams, J. Kübler, and C. D. Gelatt, Phys. Rev. B **19**, 6094 (1979).
[19] A. H. MacDonald, W. E. Pickett, and D. D. Koelling, J. Phys. C **13**, 2675 (1980).
[20] F. D. M. Haldane, Phys. Rev. Lett. **93**, 206602 (2004).
[21] X. Wang, D. Vanderbilt, J. R. Yates, and I. Souza, Phys. Rev. B **76**, 195109 (2007).
[22] A. Husmann and L. J. Singh, Phys. Rev. B **73**, 172417 (2006).
[23] E. V. Vidal, G. Stryganyuk, H. Schneider, C. Felser, and G. Jakob, Appl. Phys. Lett. **99**, 132509 (2011).